5. H. Angerstein-Kozlowska, B. E. Conway, and W. B. A. Sharp, *J. Electroanal. Chem.*, **43**, 9 (1973).
6. J. O. Zerbino, N. R. de Tacconi, A. J. Calandra, and A. J. Arvía, *This Journal*, **124**, 475 (1977).
7. A. J. Appleby, *ibid.*, **120**, 1205 (1973).
8. D. Gilroy and B. E. Conway, *Can. J. Chem.*, **46**, 875 (1968).
9. D. Gilroy, *J. Electroanal. Chem.*, **71**, 257 (1976).
10. D. Gilroy, *ibid.*, **83**, 329 (1977).
11. N. R. de Tacconi, A. J. Calandra, and A. J. Arvía, *ibid.*, **57**, 325 (1974).
12. N. R. de Tacconi, A. J. Calandra, and A. J. Arvía, *ibid.*, **51**, 25 (1974).
13. A. J. Arvía, *Anal. Quím. (Madrid)*, **71**, 944 (1975).
14. N. R. de Tacconi, J. O. Zerbino, M. E. Folquer, and A. J. Arvía, *J. Electroanal. Chem.*, **85**, 213 (1977).
15. K. Kinoshita, J. T. Lundquist, and P. Stonehart, *ibid.*, **48**, 157 (1973).
16. S. D. James, *This Journal*, **116**, 1681 (1969).
17. S. Shibata, *Electrochim. Acta*, **22**, 175 (1977).
18. T. Biegler, D. A. J. Rand, and R. Woods, *J. Electroanal. Chem.*, **29**, 269 (1971).
19. T. Biegler, *This Journal*, **114**, 1261 (1967).
20. R. Parsons and W. H. M. Visscher, *J. Electroanal. Chem.*, **36**, 329 (1972).
21. A. Kozawa, *ibid.*, **8**, 20 (1964).
22. T. Biegler and R. Woods, *ibid.*, **20**, 73 (1969).
23. Yu. M. Tyurin, G. M. Afon'shin, G. F. Volodin, and V. E. Goncharuk, *Elektrokhimiya*, **6**, 1854 (1970).
24. Yu. M. Tyurin and G. F. Volodin, *ibid.*, **6**, 1186 (1970).
25. G. F. Volodin and Yu. M. Tyurin, *ibid.*, **7**, 233 (1971).
26. L. A. Khanova, E. V. Kasatkin, and V. I. Veselovskii, *ibid.*, **8**, 451 (1972).
27. S. Schuldiner, M. Rosen, and D. R. Flinn, *Electrochim. Acta.*, **18**, 19 (1973).
28. Yu. Ya. Vinnikov, V. A. Shepelin, and V. I. Veselovskii, *Elektrokhimiya*, **9**, 552 (1973).
29. Yu. Ya. Vinnikov, V. A. Shepelin, and V. I. Veselovskii, *ibid.*, **9**, 649 (1973).
30. Yu. Ya. Vinnikov, V. A. Shepelin, and V. I. Veselovskii, *ibid.*, **9**, 1557 (1973).
31. D. A. J. Rand and R. Woods, *J. Electroanal. Chem.*, **35**, 209 (1972).
32. T. Biegler, *This Journal*, **116**, 1131 (1969).
33. A. N. Frumkin, in "Advances in Electrochemistry and Electrochemical Engineering," Vol. 3, P. Delahay, Editor, Chap. 5, Interscience, New York (1963).
34. S. Shibata, *Bull. Soc. Chim. Jpn.*, **36**, 525 (1963).
35. M. E. Folquer, N. R. de Tacconi, J. R. Vilche, and A. J. Arvía, *This Journal*, In press.
36. R. Córdova Orellana, M. E. Martins, and A. J. Arvía, *Electrochim. Acta*, In press.
37. V. I. Luk'yanicheva, L. A. Fokina, N. A. Shumilova, and V. S. Bagotskii, *Elektrokhimiya*, **13**, 1089 (1977).
38. J. A. Huang, W. E. O'Grady, and E. Yeager, *This Journal*, **124**, 1732 (1977).
39. B. Lang, R. W. Joyner, and G. A. Somorjai, *Surf. Sci.*, **30**, 440 (1972).
40. B. Lang, R. W. Joyner, and G. A. Somorjai, *ibid.*, **30**, 454 (1972).

Semiconductor Electrodes

XVII. Electrochemical Behavior of n- and p-Type InP Electrodes in Acetonitrile Solutions

Paul A. Kohl* and Allen J. Bard**

Department of Chemistry, The University of Texas at Austin, Austin, Texas 78712

ABSTRACT

The photoelectrochemical behavior of n- and p-InP single crystal semiconductors was investigated in acetonitrile (ACN) solutions which contained various electroactive compounds. The cyclic voltammograms of the semiconductors in the dark and illuminated with red light were compared to the Nernstian behavior at a Pt disk electrode. The extent of photodissolution of the semiconductors was decreased in ACN compared to aqueous solutions at similar potentials. Intermediate levels or surface states located between the conduction band and valence band which mediate electron transfer with solution redox couples are proposed. An underpotential was developed for the photo assisted oxidations and reductions with n- and p-InP, respectively, and the potential range for photoreductions on p-InP extended negative of the conduction bandedge. The electrochemical behavior and magnitude of the underpotentials is compared to results with InP in aqueous solutions and with other semiconductors in ACN.

The semiconductor-solution interface poses interesting properties which can be employed in the conversion of light energy to electrical and chemical energy by photoassisting electron transfer between the semiconductor and solution species. InP is of particular interest because its bandgap of 1.25 eV is well suited for efficient use of solar energy in a photovoltaic threshold device (1). Although InP tends to be unstable in aqueous solutions under irradiation, previous studies by Wrighton *et al.* (2) have shown that n-InP can be used as a stable photoanode for the oxidation of Te^{2-} in aqueous solutions. These authors found that while the positions of the bandedge energies and E_g for InP are similar to other semiconductors, such as GaAs (3-5), the maximum underpotential for electron transfer and the open-circuit photovoltage (V_{oc}) for stable redox systems, which reflect the fraction of the input light available as work was noticeably smaller. The basis of photoelectrochemical stabilization and magnitude of the underpotential appears to include factors other than those predicted from simple semiconductor band theory and solution redox properties.

We describe here the photoelectrochemical behavior of n- and p-InP in acetonitrile (ACN) solutions containing various one-electron redox couples. ACN has been shown to be well suited to the study of semicon-

* Electrochemical Society Student Member.
** Electrochemical Society Active Member.
Key words: photoelectricity, solar, voltammetry, energy conversion.

ductor electrochemistry because of its large solvent bandgap (~5V *vs.* ~1.5V for water) and the existence in it of a large number of reversible one-electron redox systems spanning a wide potential range (5-8). Previous papers in the series have shown that the rate of photodissolution of some semiconductors, [GaAs (5), CdS, GaP, ZnO (6), and Si (7)] is decreased in ACN and mechanistic information about the electron transfer and electrode stabilization can be obtained. Such studies have also shown that while semiconductor band theory (9) can be used to interpret the experimental results, many deviations from ideal behavior are observed which seem to be related to the specific chemical properties of each material; the less stable, smaller bandgap materials such as GaAs (5) and Si (7) show large deviations from predicted behavior. In this paper the location of the band-edges, the determination of the flatband potential (V_{fb}), and mapping of the bandgap region is discussed and the results interpreted with respect to semiconductor band theory and previously proposed models of electron transfer.

Experimental

The low resistivity single crystal semiconductors used (National Lead, Niagara Falls, New York) were polished, provided with ohmic contacts, and mounted as electrodes on glass rods as previously described (6, 8, 10). After the electrodes were mechanically polished with 0.5 μm alumina they were etched by one of the following procedures: (A) polished only; (B) etched in 6*M* HCl for 30 sec; (C) etched in 3:1:1 concentrated H_2SO_4:H_2O_2(30%):H_2O for 10 sec; (D) procedure (C) for 5 sec followed by 25 sec in 11*M* HCl and (E) etched in 5% Br_2 in methanol for 30 sec. The electrodes were then rinsed with distilled water and ethanol and then dried under vacuum for 1 hr. The purification, drying, and characterization of all other chemicals followed previously determined procedures (5-8).

A conventional three-electrode electrochemical cell fitted with an optical window was used for all electrochemical measurements. The Pt wire counterelectrode and Ag wire reference electrode were each separated from the main compartment by a medium porosity fritted glass disk. The main compartment also contained a large area Pt counterelectrode (>10 cm^2) for capacitance measurements. The cyclic voltammograms were obtained with a PAR (Princeton Applied Research, Princeton, New Jersey) Model 173 potentiostat and Model 176 Universal Programmer. The current-voltage curves were recorded on a Houston Instruments (Austin, Texas) Model 2000 X-Y recorder or a Nicolet (Madison, Wisconsin) Model 1090A digital oscilloscope for scan rates greater than 1 V/sec. The open-circuit voltage was measured with the electrometer output of the potentiostat. The semiconductors were illuminated with a 450W xenon lamp (Oriel Corporation, Stamford, Connecticut) which was fitted with a red filter (*i.e.*, wavelength >600 nm).

Results and Discussion

Flatband potential.—The V_{fb} and energy of the edges of the conduction (E_c) and valence (E_v) bands for the n- and p-InP were determined by three independent methods. First, the cell capacitance (C) was measured for potentials consistent with a depletion layer formed within the semiconductor electrode from the charging current in the cyclic voltammograms for scan rates, v, of 0.5-500 V/sec (11). A plot of C^{-2} *vs.* V produced linear Schottky-Mott plots at a given v from −0.1 to −0.8V for n-InP and −0.1 to −0.5V for p-InP, following Eq. [1]

$$C^{-2} = (V - V_{fb} - kT/e)2/(e\epsilon\epsilon_0 N_D) \qquad [1]$$

where ϵ is the dielectric constant of the semiconductor, ϵ_0, the permittivity of free space, N_D, the dopant density, e, the electronic charge, k, the Boltzmann constant, and T, the absolute temperature. Frequency dependency of the slopes and x-intercepts were observed for both materials over this range of v as discussed previously (12), and this causes some uncertainties in the derived V_{fb} and N_D values. The donor and acceptor densities were estimated as 3×10^{19} cm^{-3} and 8×10^{18} cm^{-3} for the n- and p-InP, respectively, and V_{fb} was $-1(\pm 0.2)$V (n-InP) and $0.0(\pm 0.2)$V (p-InP).

V_{fb} was also estimated from the open-circuit photovoltage (13). Briefly, when the potential of an n-type semiconductor electrode with a potential adjusted positive of V_{fb} is illuminated with light of energy greater than E_g, the open-circuit potential pulses in the negative direction toward V_{fb}. Similarly, a p-type semiconductor polarized negative of V_{fb} shows potential pulses in a positive direction, toward V_{fb}, when illuminated. The potential of the electrodes was set with a battery and negative potential pulses were observed with n-InP for potentials positive of $-1V(\pm 0.2)$ and positive pulses were observed for p-InP from −0.1 to $-2.4V(\pm 0.2V)$ in good agreement with the Schottky-Mott plot estimates of V_{fb}.

V_{fb} was also located from the most negative potential at which a photoanodic current for oxidation of an electroactive solution species was observed for n-InP and most positive photoreduction current on p-InP, as will be discussed.

Voltammetric studies.—Cyclic voltammetry (*cv*) at the semiconductor electrodes in the dark and illuminated with red light was carried out for a number of compounds and the results compared to those obtained at a Pt electrode immersed in the same solution. The peak potentials (E_p) and wave shapes were dependent upon scan rates and intensity of irradiation for the irreversible and quasi-reversible waves. The E_p values, which were generally stable and reproducible, are summarized in Table I and values obtained under irradiation are shown in Fig. 1. Details of the behavior for different couples are discussed below.

n-InP.—The background behavior of n-InP in an ACN solution containing only 0.1*M* TBAP is shown in Fig. 2a. A small reduction was observed at potentials negative of the conduction bandedge which involved ~20 μC/cm^2. A small photooxidation current was observed at potentials as far negative as −1.0V, approximately V_{fb}. However, this anodic current, which is attributed to the photodissolution, does not reach significant current densities until potentials positive of 0.0V. Redox couples with E° values (as estimated from *cv* at a Pt electrode) negative of the CB edge show nearly reversible dark *cv* i-V curves at n-InP, as expected when an accumulation layer forms, resulting in degeneracy and metal-like behavior. Previous studies have shown that n-TiO_2 (8), n-CdS and n-ZnO (6) exhibit nearly reversible *cv* behavior at potentials negative of V_{fb}. As shown in Table I, the cathodic peak potentials (E_{pc}) for A, DPA, Ox-1, $Ru(bipy)_3^{+2}$, and $Ru(TPTZ)_2^{3+}$ were nearly the same as at a Pt disk electrode and were unaffected by irradiation with red light. The current decay following the current peak, which showed $t^{-1/2}$ dependency (*i.e.*, diffusional behavior) in the dark, was affected by irradiation; this has been attributed to some convective stirring due to heating of the electrode surface. The behavior in this region was generally independent of the etchant.

Couples with E_{redox} levels located within the gap region show irreversible reduction in the dark and photoanodic currents under illumination. The reduction of AQ, whose E° lies slightly positive of V_{fb}, takes place at electrode potentials more negative than V_{fb} with the onset of degeneracy within the semiconductor (Fig. 3). The dark reoxidation of the radical anion only appeared at potentials corresponding to E_v, prob-

Table I. Peak potentials for reductions and reoxidations of the compounds used in this study at the semiconductor electrodes in the dark and illuminated with red light. All potentials are vs. SCE and at a scan rate of 0.2 V/sec*

		n-InP $V_{fb} = -1.0V$ (±0.2)				p-InP $V_{fb} = 0.0V$ (±0.2)			
		Dark		Illuminated		Dark		Illuminated	
Compound†	Pt	E_{pc}	E_{pa}	E_{pc}	E_{pa}	E_{pc}	E_{pa}	E_{pc}	E_{pa}
A	−1.94	−1.97	−1.91	−1.97	−1.91	−2.38	−1.75	−1.75	−1.62
DPA	−1.84	−2.0	−1.81	−2.0	−1.81	−2.21	−1.5	−1.65	−1.41
$Ru(bipy)_3^{+2}$	−1.30	−1.33	−1.27	−1.33	−1.27	−1.7	−0.85**	−0.85	−0.7
	−1.50	−1.53	−1.46	−1.52	−1.46	−2.19	−0.90	−1.03	−0.85
	−1.75	−1.77	−1.68	−1.76	−1.68	−2.3	−2.1	−1.38	−1.17
$Ru(TPTZ)_2^{+3}$	−0.80	−0.84	−0.74	−0.84	−0.77	−1.24	−0.44	−0.3	−0.17
	−0.97	−1.01	−0.94	−1.01	−0.95	−1.33	−0.64	−0.64	−0.41
	−1.63	−1.69	−1.56	−1.69	−1.58	−1.78	−1.5	−1.34	−1.14
	−1.87	−1.92	−1.83	−1.92	−1.83	−2.02	−1.83	−1.58	−1.39
AQ	−0.94	−1.24	0.0**	−1.24	−0.6	−1.9	0.25**	−1.5	0.25
BQ	−0.52	−0.94	0.58**	−0.77	−0.71	−1.4	—**	−0.14	−0.08
Ox − $1^{+\cdot}$	−0.42	−0.51	0.32**	−0.51	−0.59	−1.34	−0.12	−0.1	−0.08
	−1.3	−1.37	−1.15	−1.37	−1.21				
$TMPD^{+\cdot}$	0.1	−0.29	—**	−0.22	−0.07	−1.0	0.41	0.11	0.49

* Irradiation with red light; pretreatment (D), unless noted otherwise.
† Abbreviations used in this table: A, anthracene; DPA, diphenylanthracene; bipy, bipyridine; TPTZ, 2,4,6-tripyridyl-s-triazene; AQ anthraquinone; BQ, benzoquinone; Ox − 1, oxazine − 1; TMPD, N,N,N'N'-tetramethyl-p-phenylenediamine.
** Etched by procedure (E).

ably via band to band tunneling through the thin space charge region. The E_p values for AQ depended upon the etchant and the largest photoanodic currents, found with treatment (E), are reported in Table I. The photooxidation current appeared to start about −1.05V, near V_{fb}, where a depletion layer is formed within the n-InP which forces the photogenerated holes within the semiconductor to the semiconductor-solution interface to be filled by electron transfer from the $AQ^{-\cdot}$.

Redox couples whose $E°$'s are located at energies near the middle of E_g, *e.g.*, BQ and Ox − $1^{+\cdot}$, were reduced on n-InP with the E_{pc} shifted negative from its value on a Pt disk electrode, as shown in Fig. 4. However, the reduction peak occurred at potentials positive of V_{fb}, possibly via an intermediate level mechanism as previously proposed with n-TiO_2 (8), n-CdS, n-ZnO (6), n-GaAs (5), and n-Si (7). The reduced species, $BQ^{-\cdot}$ and Ox − 1 were photooxidized at potentials negative of their values on Pt; the underpotential for the photooxidation indicates the work available from the illumination as chemical or electrical energy. The magnitude of the underpotential is limited by the potential at which the reduction (or back reaction) occurs. Thus, the dark reductions which were observed at potentials positive of V_{fb} via the intermediate level, limit the output of the semiconductor threshold device. The open-circuit photovoltage, which was measured between the n-InP and a large area Pt counterelectrode in an equimolar BQ, $BQ^{-\cdot}$ (2-10 m*M*) was only about 260 mV rather than the maximum predicted value of $|E° - V_{fb}|$ of about 500 mV. Note that aqueous studies of redox systems energetically located at a similar level have shown only the dissolution of the InP at these potentials.

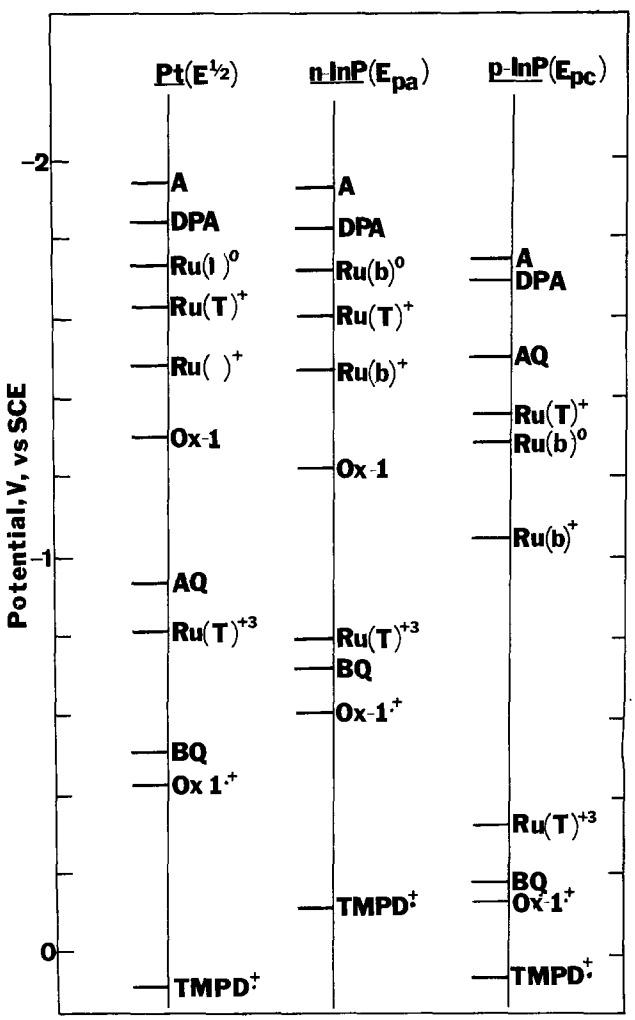

Fig. 1. Peak potentials for photooxidations on n-InP and photoreductions on p-InP.

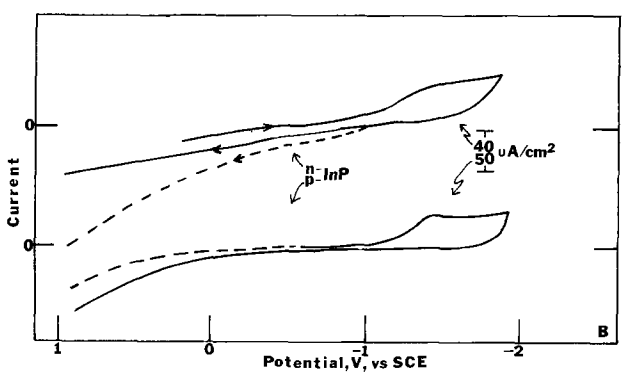

Fig. 2. Cyclic voltammogram in ACN −0.1M TBAP of n-InP and p-InP at 0.2 V/sec in the dark (——) and illuminated with red light (- - - - - -).

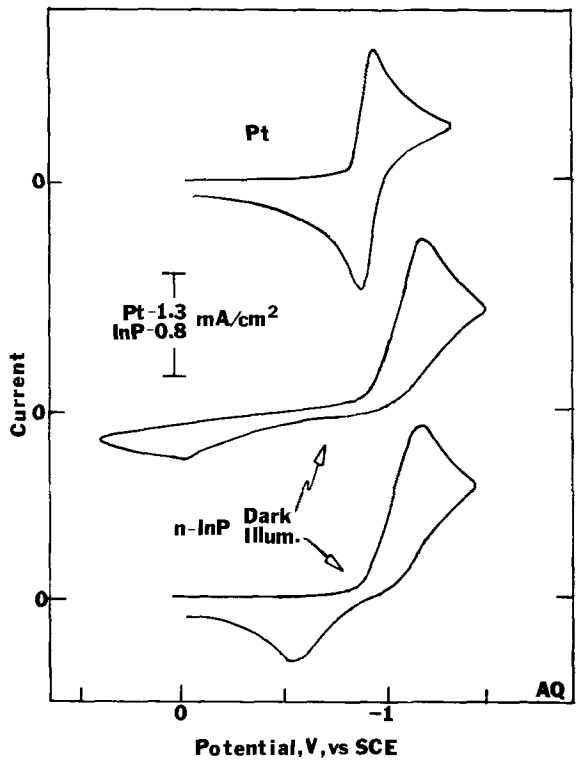

Fig. 3. Cyclic voltammogram at 0.2 V/sec of a 2 mM solution of AQ at a Pt disk electrode and n-InP electrode in the dark and illuminated with red light.

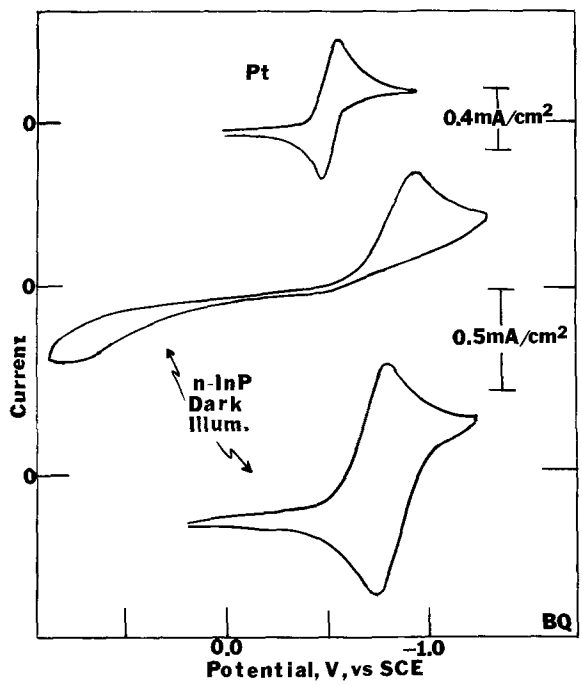

Fig. 4. Cyclic voltammogram of a 0.4 mM BQ, 0.4 mM BQ^- solution at a Pt disk and single crystal n-InP electrode in the dark and illuminated with red light; $v = 0.2$ V/sec.

The reduction of $TMPD^+$ to TMPD, which occurs reversibly at a Pt disk electrode at potentials just negative of the InP VB edge, was irreversibly reduced on n-InP in the dark at potentials well positive of V_{fb}. The photooxidation of TMPD to the blue-colored radical cation was observed at a potential of about 170 mV more negative than on a Pt disk. The extent of the negative shift in the photooxidation peak was again limited by the rate of the dark reduction.

The electrode pretreatment procedure had a significant effect on the observed behavior. Thus for AQ pretreatments (A) and (B) produced more reversible dark *cv* curves than that shown in Fig. 3; irradiation had very little effect on these. These pretreatments probably produced a large number of defects and energy levels at the semiconductor surface as a result of the abrasive polishing and the lack of sufficient etching. Treatments (C), (D), and (E) produced voltammograms more characteristic of n-type semiconductor behavior. Pretreatment (D) produced underpotentials only slightly inferior to those shown in Table I for couples in the gap region while treatments (A) and (B) again produced more reversible dark behavior (*i.e.*, peak separations similar to those on a Pt disk electrode) and very small photoeffects.

p-InP.—The background current of p-InP in an ACN solution containing 0.1*M* TBAP is shown in Fig. 2b. A small dark reduction wave was again observed and the oxidation current in the dark, corresponding to dissolution of the InP, seen at potentials positive of 0V, near V_{fb}, was decreased in magnitude under illumination with red light. More specifically, irradiation caused a decrease in the oxidation current of p-InP in the dark with a small cathodic current spike observed when the light pulse was initiated. After potential scans to +1V, where the dissolution was observed, the small reduction peak at potentials negative of −1V was much larger than in an initial cathodic scan. This suggests that products of the dissolution are reduced at these potentials. When this negative going potential sweep was carried out while the p-InP was irradiated with red light, the photoreduction started just positive of 0V, near V_{fb}, and the cathodic peak height increased.

In studies of various redox couples, pretreatment (D), which produced the largest photoassisted reduction currents and caused a slight darkening of the electrode surface was used, unless otherwise noted. Redox couples whose standard redox potentials lie negative of the CB edge are expected, from the usual band model, to be oxidized (and rereduced) with minimal photoeffects because of the potential independent rate of oxidation (9). However, we previously found that at p-GaAs photoreductions could be performed at potentials positive of their value at a Pt disk electrode (*i.e.*, with underpotentials) for redox couples located negative of this CB edge. This was attributed to the formation of a surface layer which formed a Schottky barrier with the underlying semiconductor; this junction, when illuminated, produced a photovoltage. Similar effects were observed with p-InP, *e.g.*, with anthracene (A). The E_{pc} for the reduction of A to the blue-colored radical anion in the dark was observed on p-InP at a potential more negative than that observed at a Pt disk electrode, as shown in Fig. 5a. However A was photoreduced at potentials well positive of the $E°$ for the A/A^- couple, *i.e.*, at an underpotential. At higher light intensities the cathodic peak was shifted to even more positive potentials because of the increased rate of photoreduction with respect to the fixed rate of oxidation. This photoreduction depended on the previous history of the semiconductor surface. The importance of the previously proposed film formation is shown by the experiments in Fig. 5b, where the photocurrents resulting from pulsed irradiation of an electrode held at −1.7V (240 mV positive of the $E°$ for the A/A^- couple) are given. The photoreduction currents clearly depended upon the previous history of the electrode surface. If the potential was first scanned to −1.0V (at 0.2 V/sec) and then held at −1.7, the photocathodic current peaks with diffusion-controlled ($t^{-1/2}$) decay were not observed until after several light pulses, probably because a surface film had to be formed. However a photocathodic current with a $t^{-1/2}$ decay was observed on the first light pulse, and was constant after successive light pulses, when the

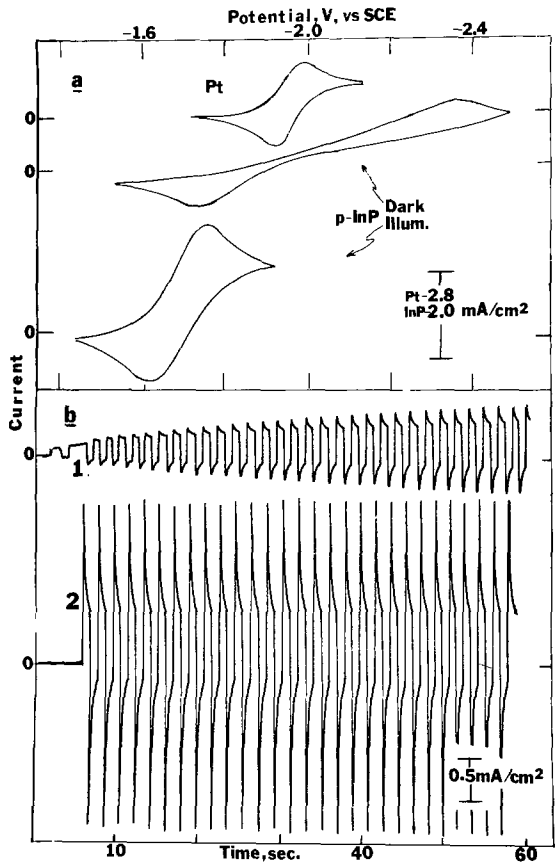

Fig. 5. (a) Cyclic voltammogram of a 2.8 mM anthracene solution at a Pt disk and p-InP electrode in the dark and illuminated with red light; $v = 0.2$ V/sec. (b) Current vs. time curve at −1.7 V of p-InP irradiated with chopped light (cathodic current plotted upward) after (1) a potential scan to −1V and (2) a potential scan to −2.2V.

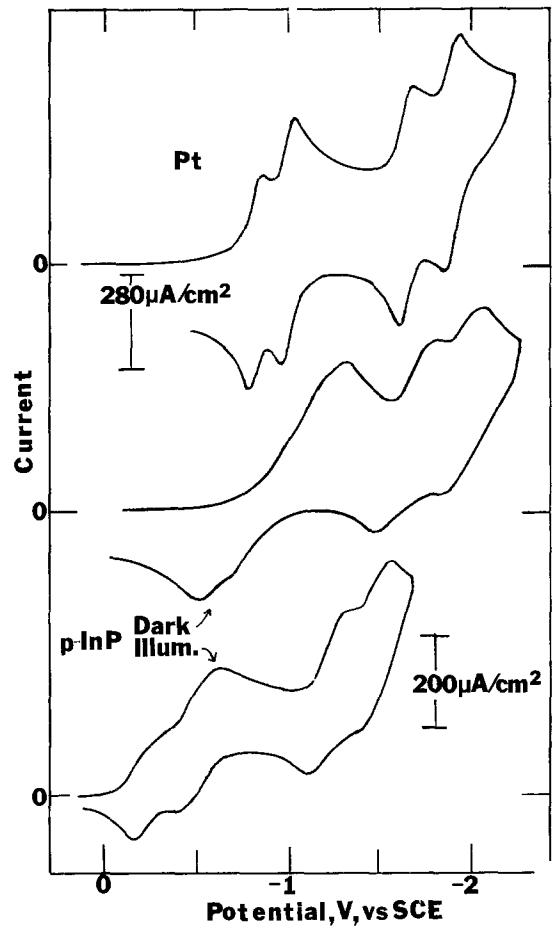

Fig. 6. Cyclic voltammogram of a 0.3 mM solution of $Ru(TPTZ)_2^{+3}$ at a Pt disk electrode and p-InP single crystal electrode in the dark and illuminated with red light; $v = 0.2$ V/sec.

electrode was first scanned to −2.2V. This behavior was reproducible and smaller photoreduction currents were again observed if the potential was again scanned to positive potentials.

The redox behavior of DPA, whose E° is also negative of the CB edge, was similar to that of A; an overpotential was observed for the dark reduction, probably because the surface film provides a barrier to electron transfer, and an underpotential was found for the reduction under irradiation. The magnitude of the underpotential was independent of E° for couples with E°'s negative of −1.3V. Thus each of the three cathodic peaks for the reduction of $Ru(bipy)_3^{+2}$ to the +1, 0, and −1 species were shifted to potentials positive of their value at Pt by a similar amount when illuminated with red light and were not shifted with respect to each other (Fig. 2). This constant photopotential can again be attributed to the voltage formed at the surface Shottky barrier.

The redox behavior of couples lying positive of the CB edge was more like that expected for the semiconductor-solution interface. The dark reduction of solution species did not occur until the potential was negative of the CB edge. In the reduction of $Ru(TPTZ)_2^{+3}$ to the anion (Fig. 6), only the Ru(III)/Ru(II) couple was located positive of the CB edge. An overpotential existed for this reduction in the dark so that E_{pc} occurred negative of −1V. The overpotential for other couples lying within E_g varied with E°, with E_{pc} always occurring negative of −1V. The reduction waves for the +1 to 0 and 0 to −1 states (Fig. 6) were both shifted by a similar amount and not with respect to one another. The oxidation of species with E°'s located within E_g, *e.g.*, AQ^-, BQ^-, $Ox - 1$, were observed at potentials more positive than V_{fb}, ~0V. The largest stable underpotential observed for the reduction of BQ to the radical anion (380 mV) was found with pretreatment (E). Although the largest photopotentials should be found for redox couples lying close to the CB edge, the rate of back reaction (*i.e.*, dark oxidation of the reduced species) limited the magnitude of the underpotential. Thus the photoreduction of $Ru(TPTZ)_2^{+3}$ started near V_{fb} but the dark oxidation limited the positive potential shift of E_{pc}. The peak potential for the photoreduction of BQ and $Ox - 1^+$ was also shifted to a similar potential under irradiation with light of energy greater than 1.25 eV. The small underpotential for the photoreduction of $TMPD^+$ is consistent with a V_{fb} located just positive of 0V *vs.* SCE.

Conclusion

This and earlier papers in this series suggest that while semiconductor band theory can be used to model the semiconductor-solution interface and form a basis for the prediction about the nature of charge transfer across it, the specific nature and properties of each semiconductor, its intermediate levels and surface behavior, must be characterized for a more complete understanding of the interface. For example, although the position of the energies of the bands are quite similar for the small bandgap semiconductors, Si, GaAs, and InP, the *i-V* curves, underpotentials, and stability in various solvents is very different. The trends in the magnitude of the underpotentials developed for the different semiconductors in ACN seem to follow that in aqueous solutions, *i.e.*, compounds such as GaAs show good solar energy conversion and stability in aqueous and nonaqueous solvents while

InP and Si, whose band structures are very similar, give relatively poor behavior. The use of nonaqueous solvents have also produced several novel semiconductor effects which could not be investigated in aqueous solutions. Thus while n-InP photodecomposes in aqueous solutions (except those containing Te^{2-}), the stability range in ACN is much larger. The extended solvent stability at negative potentials and the surface film effect allowed photoassisted electron transfer over a potential range of about twice E_g. Moreover, n- and p-type InP in ACN has recently been utilized for photoassisted electrogenerated chemiluminescence, where the irradiating red light was up-converted to violet emission (14).

Acknowledgment

The support of this research by the National Science Foundation and The Electrochemical Society (by an Edward Weston Fellowship to P.K.) is gratefully acknowledged.

Manuscript submitted July 5, 1978; revised manuscript received Sept. 21, 1978.

Any discussion of this paper will appear in a Discussion Section to be published in the December 1979 JOURNAL. All discussions for the December 1979 Discussion Section should be submitted by Aug. 1, 1979.

Publication costs of this article were assisted by the University of Texas at Austin.

REFERENCES

1. M. D. Archer, *J. Appl. Electrochem.*, **5**, 17 (1975).
2. A. B. Ellis, J. M. Bolts, and M. S. Wrighton, *This Journal*, **124**, 1603 (1977).
3. A. B. Ellis, J. M. Bolts, S. W. Kaiser. and M. S. Wrighton, *J. Am. Chem. Soc.*, **99**, 2848 (1977).
4. K. C. Chang, A. Heller, B. Schwartz, S. Menezes, and B. Miller, *Science*, **196**, 1097 (1977).
5. P. A. Kohl and A. J. Bard, *This Journal*, **126**, 59 (1979).
6. P. A. Kohl and A. J. Bard, *J. Am. Chem. Soc.*, **99**, 7531 (1977).
7. D. Laser and A. J. Bard, *J. Phys. Chem.*, **80**, 459 (1976).
8. S. N. Frank and A. J. Bard, *J. Am. Chem. Soc.*, **97**, 7427 (1975).
9. (a) H. Gerischer in "Physical Chemistry: An Advanced Treatise," Vol. 9A, H. Eyring, D. Henderson, and W. Jost, Editors, Academic Press, New York (1970); (b) H. Gerischer, *Adv. Electrochem. Electrochem. Eng.*, **1**, 139 (1961).
10. P. A. Kohl, S. N. Frank, and A. J. Bard, *This Journal*, **124**, 225 (1977).
11. R. N. Noufi, P. A. Kohl, S. N. Frank, and A. J. Bard, *ibid.*, **125**, 246 (1978).
12. (a) E. C. Dutoit, R. L. Van Meirhaege, F. Cardon, and W. P. Gomes, *Ber. Bunsenges. Phys. Chem.*, **79**, 1206 (1976); (b) W. P. Gomes and F. Cardon, *ibid.*, **74**, 432 (1970); (c) R. A. L. Vanden Berghe, F. Cardon, and W. P. Gomes, *ibid.*, **77**, 290 (1973); (d) *ibid.*, **78**, 331 (1974); (e) A. M. Van Wezemael, W. H. La Fleve, F. Cardon, and W. P. Gomes, *J. Electroanal. Chem.*, **87**, 105 (1978).
13. V. A. Myamlin and Y. V. Pleskov, "Electrochemistry of Semiconductors," Plenum Press, New York (1967).
14. J. D. Luttmer and A. J. Bard, *This Journal*, **126**, 414 (1979).

Semiconductor Electrodes

XVIII. Liquid Junction Photovoltaic Cells Based on n-GaAs Electrodes and Acetonitrile Solutions

Paul A. Kohl* and Allen J. Bard**

Department of Chemistry, The University of Texas at Austin, Austin, Texas 78712

ABSTRACT

Regenerative photoelectrochemical cells (PEC) were constructed utilizing single crystal n-GaAs in acetonitrile solutions. Solution redox couples (anthraquinone, p-benzoquinone, dimethyl ferrocene, ferrocene, hydroxymethyl ferrocene, and tetramethyl-p-phenylenediamine) whose standard redox potential varied by over 1.2V, were photooxidized at the semiconductor electrode and reduced at a Pt counterelectrode converting light directly into electrical energy. A power conversion efficiency of 14% was observed for the n-GaAs electrode in a ferrocene-ferricenium acetonitrile solution at a radiant intensity of 0.52 mW/cm^2 of 720-800 nm light. The efficiency and stability were found to be very dependent upon the residual water concentration, radiant power, and concentration of electroactive species.

The effective utilization of semiconductor electrodes in photoelectrochemical devices for the conversion of light energy to chemical and electrical energy depends upon a knowledge of the mechanism of charge transfer at the interface and hence of the energy level distributions within the semiconductor and solution. These determine the rates of competitive reactions of photogenerated holes or electrons and thus the stability, efficiency, and over-all electrochemical behavior of the semiconductors. The characteristics of a photoelectrochemical cell (PEC) can be predicted from the electrochemical behavior of the individual semiconductors and counterelectrode in regenerative PEC's (or liquid junction photovoltaic cells) which show no net solution reaction and convert light to electricity, photoelectrosynthetic cells, which cause a net change in the solution composition and creation of chemical free energy (*e.g.*, the decomposition of water to H_2 and O_2), or in photocatalytic cells in which light is used to catalyze solution reactions at the semiconductor surface. Although a number of aqueous photovoltaic cells have been described, the recent cell by Tsubomura *et al.* (1) utilizing n-CdS and iodide ion in acetonitrile (ACN) is the only reported PEC using an aprotic solvent.

Previous studies of the electrochemical behavior of n- and p-type GaAs in anhydrous ACN solutions have shown that these semiconductors are stable under irradiation and suggested several suitable couples for use in photovoltaic PEC's (2). It was shown that:

* Electrochemical Society Student Member.
** Electrochemical Society Active Member.
Key words: energy conversion, liquid photovoltaic, solar.